



Developing Test Methods for Compression after Lightning Strikes

Xiaodong Xu^{1,2} · Scott L. J. Millen³ · Juhyeong Lee⁴ · Gasser Abdelal³ · Daniel Mitchard⁵ · Michael R. Wisnom² · Adrian Murphy³

Received: 8 August 2022 / Accepted: 21 December 2022 / Published online: 25 January 2023
© The Author(s) 2023

Abstract

Research into residual strength after lightning strike is increasing within the literature. However, standard test methods for measuring residual compressive strength after lightning strikes do not exist. For the first time, a systematic experimental study is undertaken to evaluate modifications necessary to standard Compression After Impact (CAI) specimen geometry and test jig design to induce specimen failure at the lightning damage region. Four laboratory generated lightning strike currents with peak amplitudes ranging from 25 to 100 kA have been studied. Test set-up modifications were made considering the scale of the lightning damage and its potential proximity to specimen edges. Specimen geometry and anti-buckling guides were adjusted for each peak current to induce specimen failure at the lightning damage. The Compression After Lightning (CAL) strength was 28% lower than the pristine CAI strength even at a relatively low peak current of 25 kA. This study shows that the standard CAI test setup has the potential for CAL application, however, careful modifications are required depending on the peak amplitude of the applied lightning current waveform.

Keywords Laminate · Strength · Compression after impact · Lightning strike

1 Introduction

1.1 Lightning Strike Experiments

Composite materials, through ever increasing use in primary aircraft structures, produce weight reduction and improved fuel efficiency over legacy metal airframes. However, composite

✉ Xiaodong Xu
xiaodong.xu@uwe.ac.uk

¹ University of the West of England, Coldharbour Lane, Bristol BS16 1QY, England, UK

² Bristol Composites Institute, University Walk, Bristol BS8 1TR, England, UK

³ School of Mechanical and Aerospace Engineering, Queen's University Belfast, Stranmillis Road, Belfast BT9 5AH, Northern Ireland, UK

⁴ Department of Mechanical and Aerospace Engineering, Utah State University, Logan, UT 84322-4130, USA

⁵ Advanced High Voltage Engineering Research Centre, School of Engineering, Cardiff University, Cardiff, CF24 3AA Wales, UK

structures are more susceptible to lightning strike damage due to their relatively low electrical conductivities. Lightning strikes have been standardised into four discrete waveforms, A-D, presented in SAE-ARP5412B and its European equivalent, EUROCAE ED-84, each with different peak current profiles [1, 2]. Waveform A is characterised as the first return stroke; Waveform B is the intermediate current; Waveform C is the long duration, low current; and Waveform D is a subsequent stroke. A sizeable amount of experimental research has been conducted on lightning strike damage in a laboratory environment and has typically focussed on the high peak current Waveforms A or D [3–11]. The typical peak natural lightning current amplitude is around 30 kA but can exceed 100 kA. The 25 to 100 kA peak current test (corresponding to Waveform D) is the most frequently used in a laboratory environment and the 100 kA peak current is usually considered a worst-case scenario. This ensures that components are over-engineered for some of the most extreme lightning currents they may experience [10]. Experimentally, authors have studied the influence of novel Lightning Protection Systems (LSPs) [12–17], sequential strikes using multiple waveforms [18] or single strike tests [19]. Research on simulating the direct effects of lightning (physical damage) have predominantly focused on the thermal-electric effect in the specimen due to resistive or Joule heating [18, 20, 21]. A smaller number of works have considered dynamic mechanical pressure loading [22–24], thermal expansion [25, 26] or a combination of these effects [25–27].

Lightning damage in typical fibre composites can be characterised as fibre fracture (blow-out or tow splitting), matrix cracking and decomposition, and delamination [28]. Visual inspection of physical lightning damage on composites typically identifies surface damage areas including matrix thermal decomposition combined with broken and frayed fibres. Non-Destructive Testing (NDT) methods are used to characterize intralaminar matrix cracking and delamination. Significantly, lightning damage is often reported to be at and close to the outermost plies. This is frequently in contrast to studies with mechanical impact damage, for example dropped weight impact, where damage occurs through the entire thickness or only at the side opposite to the impact event due to stress wave transmission/reflection [29–31]. Several authors have studied residual strength of composite laminates after laboratory generated lightning strike, compared these with dropped weight impact, and have found very different damage morphologies and structural responses [5, 32, 33]. However, damage from both events can significantly reduce the residual strength of the structure [4, 7, 12, 34–41].

1.2 Experimental Lightning Strike Residual Strength Assessment

Few works which conducted lightning strikes on composite structures have studied the residual strength of composite laminates post-strike [4, 7, 34–43]. Many authors have used either three-point [36–40] or four-point [12, 41] flexural testing to assess residual strength. However, this form of testing, with the laminate being loaded normal to the reinforcing fibres, in the region of the damage, is less representative of design in large and high-performance structures. To date, few works are available which have examined specimens' residual strength under more representative laminate in-plane tensile [35] or compressive [34, 44] loading. All these experimental works are summarised in Table 1. Independent of the loading, many of these works have established relationships between peak current and residual strength [4, 40, 45]. In general, increasing peak current has been shown to reduce the residual strength of the laminate. For example, Wang et al. [46] found that composite laminate residual tensile strength was greater than 80% after a 60 kA lightning strike, with residual strength decreasing progressively at higher peak currents.

Most recent works conducting residual strength assessments after lightning strike have determined the residual strength of unprotected CFRP specimens and specimens protected with LSPs [7, 12–14, 19, 41, 46–50]. Hirano et al. [12] compared the residual strength of unprotected CFRP and those protected with intrinsically conducting polyaniline (PANI) polymer. Residual strength was examined after a simulated 100 kA peak lightning current, while an unprotected specimen was tested at 40 kA. Results showed that the protected specimen suffered only a 10% reduction in residual strength, while the unprotected specimen residual strength reduced by 76%, even with a lower peak current. Many of these works found that using LSP could retain more than 97% of the specimen's pristine strength.

1.3 Compression After Impact (CAI) Test Method

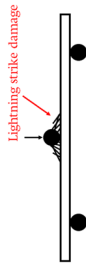
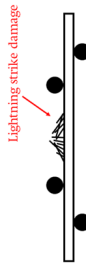
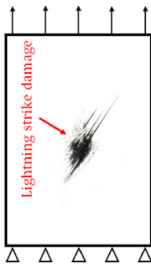
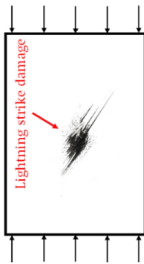
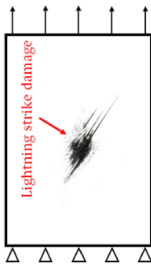
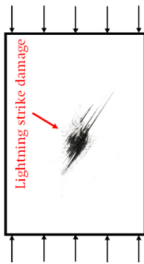
Only four of the papers listed in Table 1 consider in-plane tensile or compressive residual strength [4, 15, 19, 46]. In contrast, low velocity impact and the effects of impact damage in laminated composites were intensively investigated in the past, as reviewed by Abrate [51]. CAI strength is a key design driver for composite structures subject to kinematic impact and the CAI strength can be related to the internal damage area [52]. Sun and Hallett [53] studied CAI strength after quasi-static indentation and low velocity impact and highlighted the importance of understanding the internal damage such as matrix cracks and delamination. X-ray Computed Tomography (CT) is extremely helpful in understanding such internal damage. It was successfully demonstrated by Nettles and Scharber [54] who concluded that the Mode II fracture toughness had a significant effect on delamination area which then correlated directly to CAI strength.

To date, few attempts have been made to adopt a standard CAI test method for measuring residual compressive strength after lightning strikes. Wang et al. [34] subjected 500 mm × 250 mm × 2 mm specimens to 93.7 kA Waveform A and D lightning tests before completing CAL tests using a compression arrangement inspired by the standard CAI jig. However, the use of long, thin specimens produced undesirable failure modes such as compressive failure away from the lightning damage zone due to buckling.

1.4 Summary

A small body of research has been conducted to determine the residual strength of composite specimens after lightning strike with various waveforms, peak currents, and protection layers. Peak current has been directly correlated with residual strength considering tensile, compression and flexural loading, of both complete specimens and sectioned sub-specimens. Several works have additionally drawn a connection between the general scale of lightning strike direct damage and the witnessed reduction in residual strength. Significantly only few papers [4, 15, 19] have considered in-plane compressive residual strength, and in these works non-standard test arrangements were used and some undesired specimen failure modes were observed. It is also well known that the CAI test is notoriously difficult to perform successfully [52]. Therefore, since there is very limited CAL work in the existing literature it is beneficial to investigate the difficulties and challenges associated with developing a standardised CAL test arrangement. Therefore, this paper will undertake a systematic experimental study to evaluate modifications necessary to standard CAI specimen geometry and test jig design to induce specimen failure at the lightning damage. The CAL tests will consider modifications to the standard CAI test method, and these will be used to test specimens which have been subjected to

Table 1 Summary of post-strike residual strength testing methods

Testing method	Waveform details	Material system	Specimen size	Specimen layup	Ref.(s)
Three-point flexural testing		Plain-woven	150 mm × 150 mm	[0/90] ₈	[47]
		Uni-directional	150 mm × 150 mm	[0/90] _{2s}	[48]
Four-point flexural testing		Glass fibre woven fabric	100 mm × 40 mm	[45/0/-45/90] _{2s}	[13]
		Short fibre thermoplastic	80 mm × 12.7 mm	[not stated]	[49]
In-plane tensile testing		Glass fibre composites	100 mm × 15 mm	[not stated]	[14]
		Plain-woven	150 mm × 150 mm	[0/90] ₈	[12]
In-plane compressive testing		Uni-directional	120 mm × 35 mm	[45/0/-45/90] _{2s}	[41]
		Uni-directional	305 mm × 38 mm	[45/0 ₂ /-45/0 ₃ /90] _s	[4]
In-plane compressive testing		Uni-directional	120 mm × 35 mm	[45/90/-45/0] _s	[46]
		Silver modified buckypaper-carbon fibre	360 mm × 360 mm	[0/90] _{1,6s}	[15]
In-plane compressive testing		Uni-directional	305 mm × 38 mm	[45/0 ₂ /-45/0 ₃ /90] _s	[4]
		88.4 kA, 93.7 kA and 31.3 kA, Wav. A and D	500 mm × 250 mm	[45/-45/0 ₂ /45/90/-45/0] _s	[19]

Waveform D strikes with four different peak currents. The key contribution of this work is to develop a new CAL test method and inform the research community of the advantages and disadvantages of using a standard CAI jig for CAL tests, given the lack of literature on this topic.

2 Experimental Set-up

2.1 Material and Layup

The material used in these tests was Hexcel's HexPly[®] IM7/8552 carbon/epoxy pre-preg with a nominal ply thickness of 0.125 mm. The stacking sequence was quasi-isotropic [45/90/-45/0]_{4s} for all specimens. The nominal overall thickness was 4 mm. A large test panel was designed (650 mm × 440 mm) and was struck in four quadrants to ensure material homogeneity and uniformity in manufacture. Figure 1 shows the schematic of the test specimen between the reinforced stainless-steel frame underneath and a white stainless-steel frame on top to distribute the loading pressure. Holes were drilled along the short edges and the specimen was bolted through these holes to securely fix the test specimen between the top and bottom frames. Figure 1b shows the dimensions of the top and bottom clamping frames and the resulting test area. This test area (500 mm × 440 mm) was then sectioned into four quadrants, one for each lightning test. Ideally, multiple lightning strike tests should be done at each current, but due to the cost and complexity of lightning tests and the current lack of data, valuable information can still be obtained with single strike tests in the current study.

2.2 Lightning Test Set-up

The test specimen was bolted into a grounded rig at two opposite short sides below a high voltage electrode as shown in Fig. 2. This clamping arrangement was chosen since the specimen was longer and narrower than the testing rig. The bolted connection along both short edges maintains firm and tight contact between the specimen and the grounding clamps. The purpose of the bolts is to ensure tight contact between the specimen surfaces and the

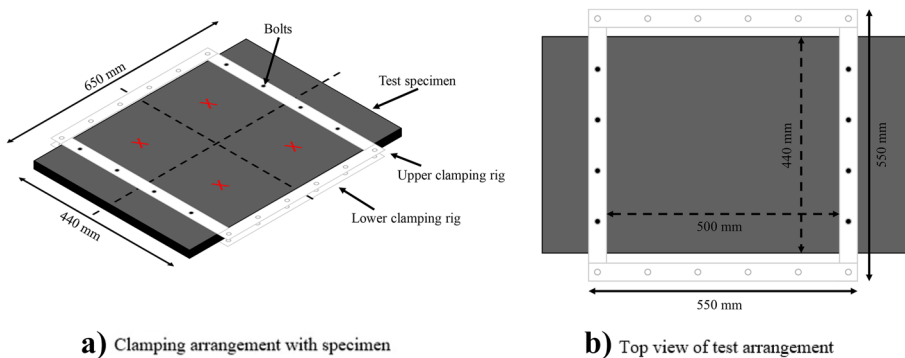
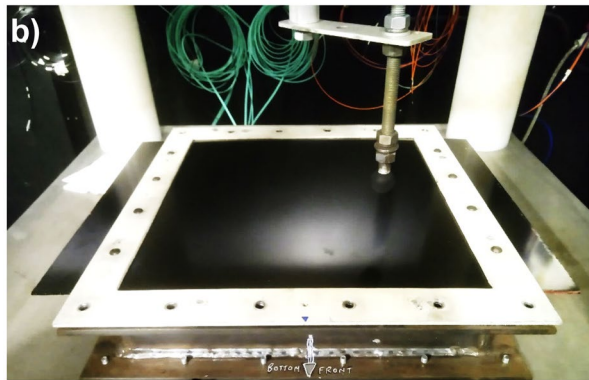
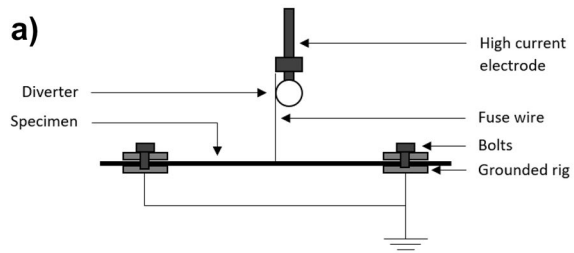


Fig. 1 Lightning specimen **a)** in the test bed (strike points shown with red x's), and **b)** its clamping arrangement

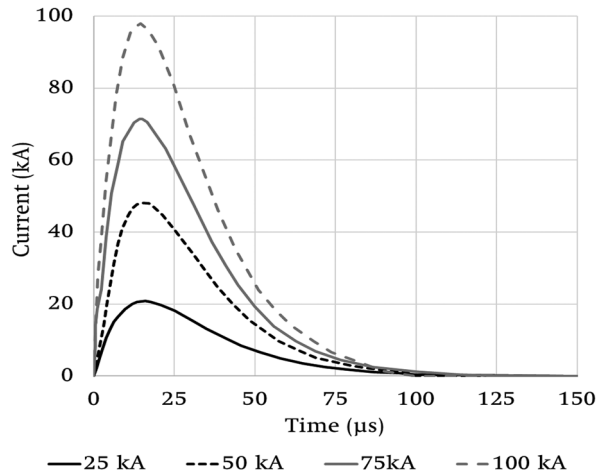
Fig. 2 Laboratory generated lightning strike test arrangement, **a)** labelled schematic, **b)** image of specimen in setup before test



grounding clamps, which is the primary route to ground for the injected specimen current. A very small fraction of the induced current may flow through the bolts from the specimen to the grounding clamps, but any such local effects are between the grounding upper and lower clamp and relatively far from the lightning attachment point (approximately 150 mm). The bolts have a small diameter (~ 8 mm) and the bolt holes will not be within the final post-strike test specimens. The drilling process is not expected to have any tangible effect on the mechanical properties of the specimen and resulting CAL strength. The use of different electrode sizes and shapes have been studied within the literature and this has been shown to affect the size of the predicted lightning damage [55–57]. Therefore, in this work to minimise variability, a small insulating plastic sphere, known as a diverter, was used to minimise any material being blown from the electrode onto the sample surface during the experiment, and a thin metallic fuse wire was used to guide the lightning arc to the exact point as required on the sample. The fuse wire, with a gap distance of 50 mm, instantaneously atomises during the initial stages of the arc formation and has no effect on the current flow or damage to the specimen.

A series of lightning strike tests were performed at the Lightning Laboratory, part of the Advanced High Voltage Engineering Research Centre of Cardiff University. A lightning generator capable of producing a Waveform D with a maximum peak current of 100 kA was used. The electrode was positioned above the centre of Quadrant 1 (Q1) and the fuse wire attached from the electrode to the centre of the quadrant to ensure that the centre was struck. A D-waveform lightning current was then injected into the sample. The electrode was then positioned above Quadrant 2 (Q2), a fuse wire attached, and 50 kA injected. This was repeated for Quadrant 3 (Q3) for 75 kA, and Quadrant 4 (Q4) for 25 kA. Feraboli and Miller [4] used a specimen only 38.1 mm wide exposed to Waveform D with peak currents of 10, 30 and 50 kA. Therefore, the

Fig. 3 Four laboratory generated D lightning waveforms with different peak currents



use of 250 mm×220 mm quadrants should be sufficient to contain the damage of the current waveforms used in this study. Figure 3 presents the injected current waveforms, showing slightly lower peak currents than the stated values. For example, the 25 kA waveform has an actual peak current of 21 kA. However, for convenience the four waveforms will be referred to as 25, 50, 75 and 100 kA throughout this paper. After these experiments, the specimen was carefully cut into its respective quadrants using a diamond-coated disk for further analysis.

2.3 Compression After Impact Test Set-up

Previously, two CAI jigs (Fig. 4) modified from the standard CAI test jig [58] were successfully used to study the strength scaling in notched compression tests [59]. These jigs were selected for this study because their design would enable easy accommodation of a wide range of specimen dimensions from 120 to 220 mm in width. Unlike the standard CAI test boundary conditions, steel jaws were used in the smaller rig to clamp the top and bottom ends of the specimen over a width of 100 mm. Anti-buckling guides were then used to gently constrain the slightly wider specimen (Fig. 4a). The purpose of these modifications was to reduce the risk of global buckling when using large specimens with lightning damage, which may initiate failure at higher load than impact damage (which the rigs were originally designed for). Therefore, this smaller modified CAI jig can be used to adapt to the range of damage resulting from the artificial lightning strikes. The same clamping modification cannot be made to the larger jig (Fig. 4b) due to the limited width of the steel jaws of 100 mm. The modification to the larger jig is only to its size.

3 Test Results

An initial inspection of the lightning damage to specimens showed many broken, lifted, and separated fibres and a large amount of surface pitting around the strike area (Fig. 5). As the peak current amplitude increased, the damage appeared to penetrate deeper into the

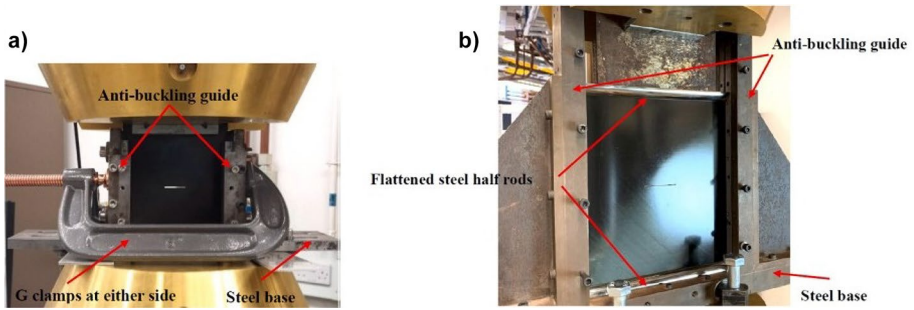


Fig. 4 Modified CAI jigs [59]: **a)** 120 mm wide notched specimen clamped to the test machine and **b)** 220 mm wide notched specimen edge-loaded

sample, with many damaged fibres and more surface pitting extending further from the lightning attachment location.

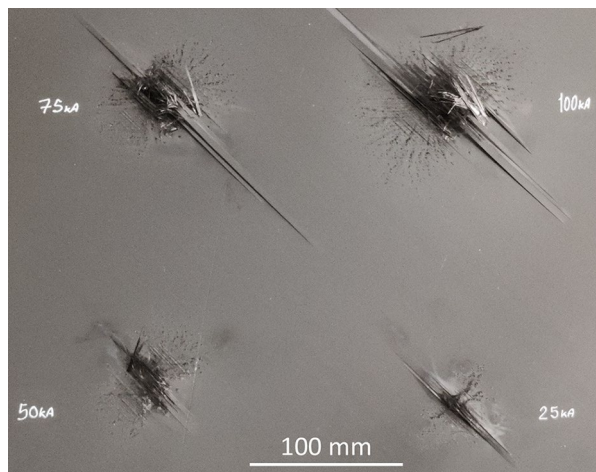
The design of appropriate CAL test methods for each artificial lightning waveform was to be informed by the CT analysis of the lightning damage states found in each of the quadrant specimens.

3.1 CT Images

Prior to CT scanning, the samples from the lightning tests were soaked in a bath of zinc iodide penetrant for 3 days. A Nikon XT H 225ST CT scanner was used to scan the sub-divided large test panel. The scanner had a 3-micron focal spot size and 225 kV, 225 W microfocus X-ray source.

The CT images taken through the specimen thickness, in Fig. 6, show the extent of damage in each sub-divided large test panel section and how this varies with peak current amplitude. These damage profiles dictate the CAL specimen dimensions by showing the extent of the maximum in-plane internal lightning damage through the thickness after lightning strikes at 100, 75, 50 and 25 kA peak currents, respectively. The internal damage did not reach the specimen edges so the damage in the four quadrants could not overlap in the panel.

Fig. 5 Composite panel after lightning strikes (25–100 kA peak currents)



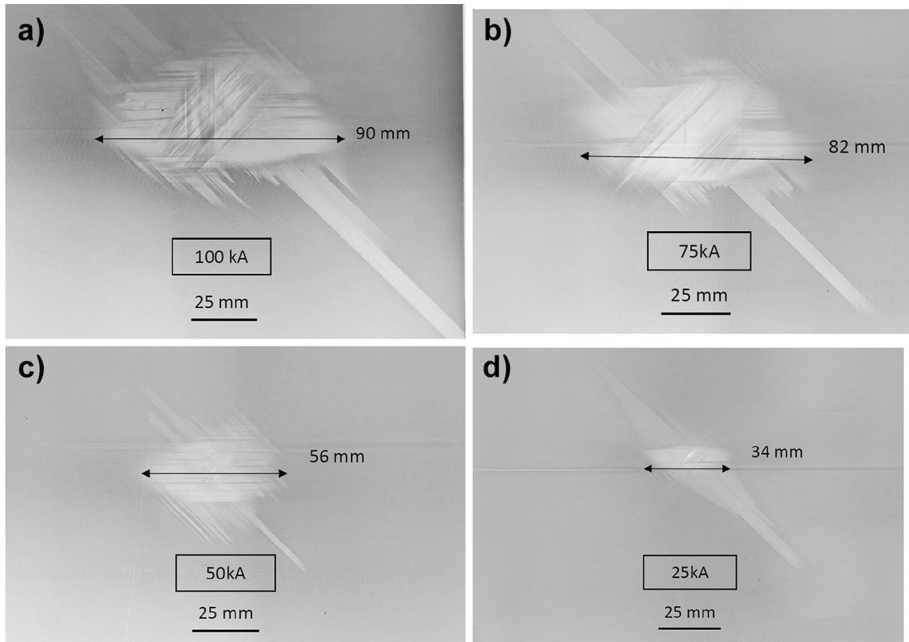


Fig. 6 CT images showing extend of internal damage after lightning strikes with a peak current of **a)** 100 kA, **b)** 75 kA, **c)** 50 kA, and **d)** 25 kA, respectively

The lowest current is expected to have the highest residual compressive strength, so the 25 kA case (Fig. 6d) is believed to be the hardest to test under compression. Therefore, CAL tests were conducted in decreasing order of peak current (100 to 25 kA) and hence decreasing damage volume to converge on an experimental design suitable for the range of peak currents.

3.2 CAL Test Result of the 100 kA Peak Current Specimen (220 mm × 220 mm)

The CAL specimen for the 100 kA peak current had to be large enough such that the damage area did not reach the edge of the specimen. The internal damage area was around 90 mm wide, therefore too close to the 100 mm standard CAI specimen width. When cutting down the specimen, the internal damage is also invisible, so it is extremely hard not to interfere with the lightning damage area during cutting with only 5 mm margin on either side. Therefore, the test panel was cut into a CAL specimen of 220 mm × 220 mm with the lightning damage centred at the horizontal and vertical midpoint of the specimen. Another option would have been to ignore the surface damage and cut the specimen to the standard size. However, this would have resulted in damage at the CAI specimen edge or within or near the compression test boundary conditions. In this case, damage could be expected to influence failure of the specimen in compression and the surface damage disproportionately impact the performance of the specimen. This resulted in a distance greater than 65 mm between the edge of the internal lightning damage and the edge of the specimen based on Fig. 6a. In this case the only change to the standard CAI test procedure, outlined in ASTM D7137 [58], was the specimen geometry.

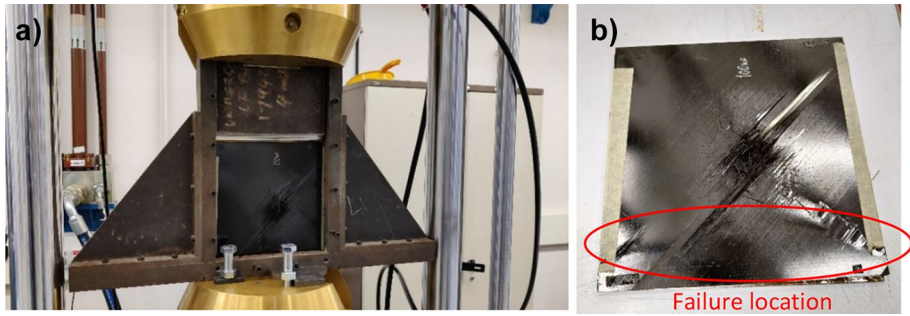


Fig. 7 100 kA CAL test a) set-up and b) failed edge-loaded specimen

The lightning damage did not initiate specimen failure and the specimen loading increased to a point where excessive out-of-plane bending was observed due to buckling. This caused an undesirable failure mode near the edges of the specimen (220 MPa, gross section), shown in Fig. 7b. It is speculated that because the lightning damage did not initiate specimen failure at a lower load, additional clamping constraints at both edges would have been necessary to eliminate the buckling behaviour and result in a direct damage-initiated material failure. This result is seen as undesirable. Smaller specimens and more constraints could reduce the tendency of buckling.

3.3 CAL Test Result of the 75 kA Peak Current Specimen (120 mm × 150 mm)

Given the challenges observed with the 100 kA specimen, the 75 kA peak current specimen was cut down to 120 mm × 150 mm. This made the specimen closer to the standard CAI size of 100 mm × 150 mm. This could be achieved because the lightning damage area was smaller for the 75 kA peak current lightning strike. This resulted in a distance greater than 19 mm between the edge of the internal lightning damage and the edge of the specimen based on Fig. 6b. However, the surface delamination was more extensive and reached the specimen edges as shown in Fig. 8a. The top and bottom edges of the specimen were also clamped to the test machine. It was expected that both measures (cutting down the specimen and specimen clamping) could reduce the tendency for buckling and out-of-plane bending. Failure occurred between the lightning damage and the end of the anti-buckling guides (264 MPa, gross section), shown in Fig. 8b. Because the failure location was at the unsupported gap in the jig but not at the specimen centre, this result was undesirable.

3.4 CAL Test Result of the 50 kA Peak Current Specimen (120 mm × 150 mm)

Given that the damage area decreased again for the 50 kA peak current specimen, the same specimen size as the 75 kA specimen could be used, 120 mm × 150 mm. This resulted in a distance greater than 32 mm between the edge of the internal lightning damage and the edge of the specimen based on Fig. 6c. It was expected that the failure load would be higher, but this was not the case (267 MPa, gross section), shown in Fig. 9. Failure was away from the lightning damage and at the end of the anti-buckling guide. This again highlights the limitation of the present CAI set-up as the lightning damage did not initiate specimen failure. Specimen failure was initiated where there is a small gap between the

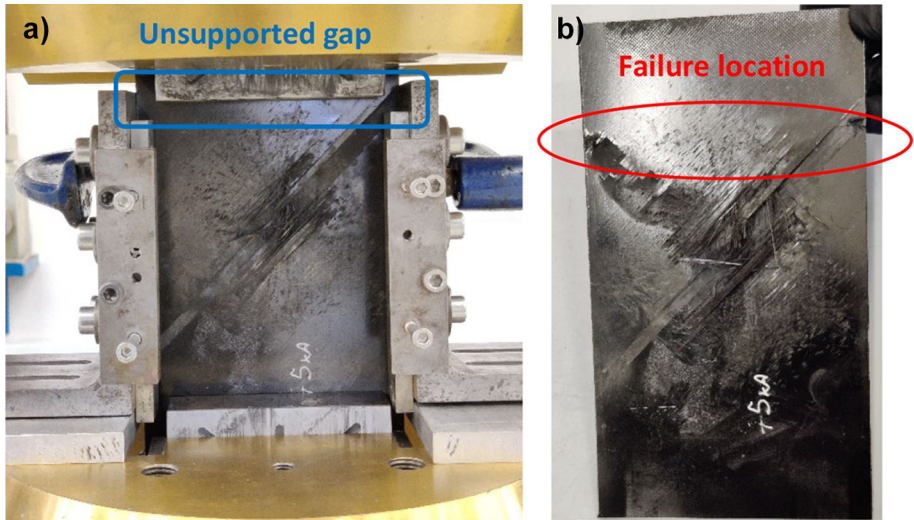


Fig. 8 75 kA CAL test a) set-up with an unsupported gap and b) failed clamped specimen

upper loading point (grips in the current set-up) and the edge of the anti-buckling guides. The combination of compression, buckling and an unsupported gap at the corner of the specimen, initiated failure. Therefore, this setup and result was seen as undesirable. Additionally, given that the failure stress was like the preceding 75 kA specimen it confirms that the preceding test was undesirable due to buckling.

3.5 CAL Test Result of the 25 kA Peak Current Specimen (120 mm × 150 mm)

The damage area was smallest for the 25 kA specimen, therefore, the specimen was kept the same as the 75 kA and 50 kA peak current specimens (120 mm × 150 mm). This resulted in a distance greater than 43 mm between the edge of the internal lightning damage and the edge of the test rig boundary conditions based on Fig. 6d. Since the delamination was smallest, the expected failure load was highest. To avoid producing the same undesirable failure modes as the preceding tests, further modifications were made to the CAI jig. The previous unsupported gap was therefore eliminated. This was only possible by using a slightly wider specimen than the CAI standard, allowing the steel jaws to move down further without touching the anti-buckling guides. All edges of the specimen were constrained throughout the test. Failure was right in the specimen centre at the lightning damage (317 MPa, gross section), as shown in Fig. 10. The mode of failure indicates that this was a successful test.

4 Results Analysis

A summary of the reduction in CAL strength from a pristine composite specimen to a specimen subjected to 25–100 kA peak current strikes is shown in Fig. 11. The 25 kA specimen is 28% weaker than the pristine CAI strength (438 MPa [52]) of the same material and

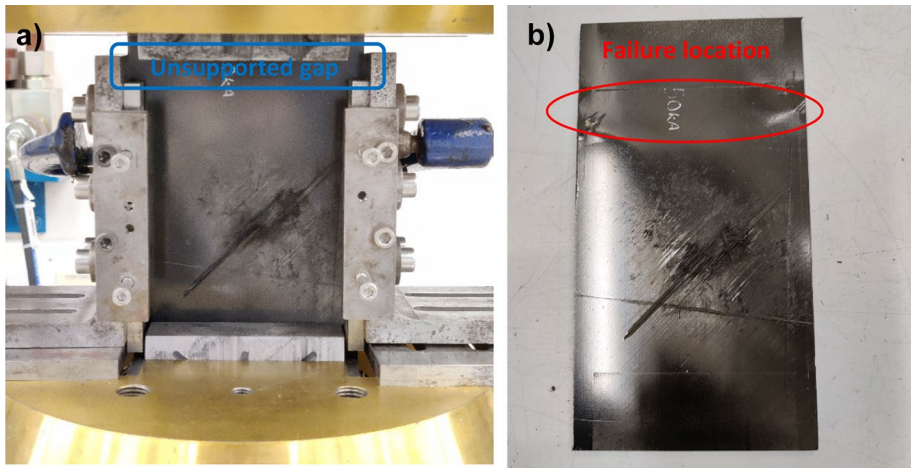


Fig. 9 50 kA CAL test a) set-up with an unsupported gap and b) failed clamped specimen

a quasi-isotropic layup owing to the presence of lightning damage. The tests with higher peak currents were undesirable due to buckling and failure location at the unsupported gap in the jig, not at the specimen centre.

5 Discussion

A set of divergent requirements have been demonstrated, where the 100 kA peak current loading resulted in damage which was greater than the standard CAI specimen size (100 mm × 150 mm), and 75 and 50 kA loading resulted in damage which did not initiate failure at the lightning damage

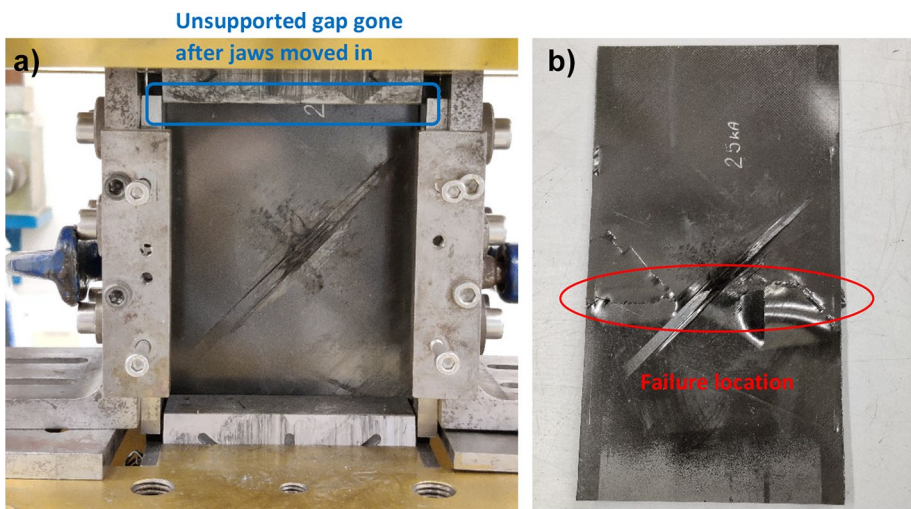
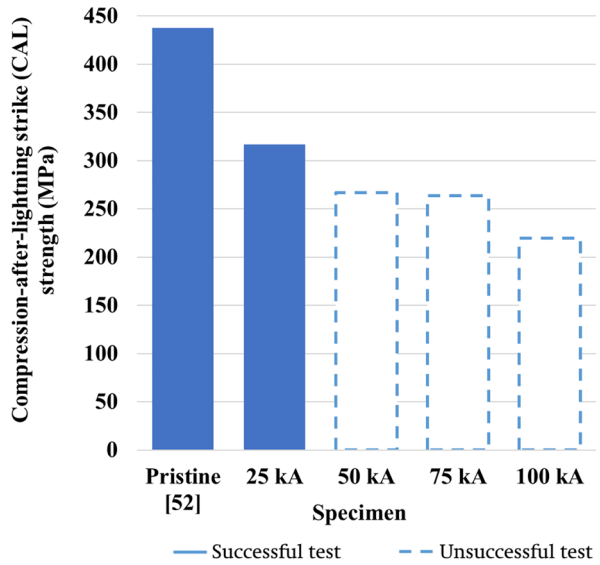


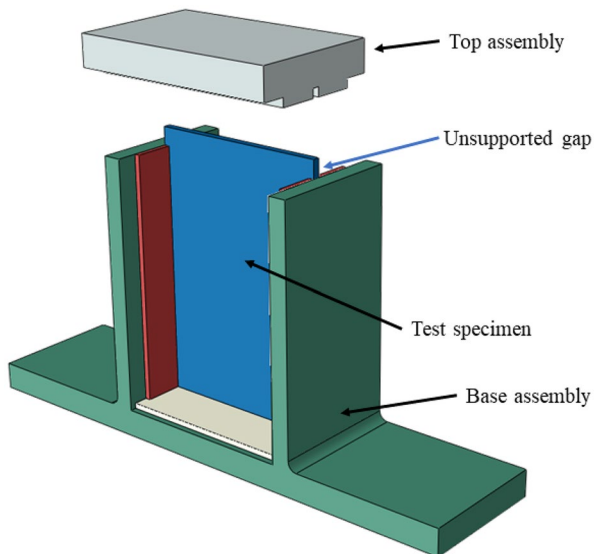
Fig. 10 25 kA CAL test a) set-up without unsupported gaps and b) failed clamped specimen

Fig. 11 Reduction in CAL strength from pristine to 25 kA peak current specimens



area before failure occurred at the test boundary conditions. As shown in Fig. 12 [58], there is an unsupported gap in the CAI jig which may initiate failure first if the damage in the test specimen does not initiate failure below 264–267 MPa for the tested combination of composite material and laminate stacking sequence. When this weakness in the setup was removed, the CAL strength for the selected material and laminate with damage from an artificial lightning strike with a peak current of 25 kA was found to be 317 MPa. These modifications effectively changed the failure location from the undesirable specimen edge to the centre, at the lightning damage region.

Fig. 12 ASTM D7137/D7137M standard [58] set-up with an unsupported gap



This represents a 28% reduction when compared with a CAI pristine strength of 438 MPa which was influenced by buckling [52]. The reported compressive strength of the same material with a quasi-isotropic layup is 666 MPa [60] using smaller specimens free from buckling. Although either of the above compressive strength values could be used as the baseline, the CAI pristine strength was chosen because it shares similar boundary conditions as the current CAL tests. Feraboli and Miller [4] reported a 15% compressive strength reduction for composite laminate subjected to a 30 kA peak current Waveform D lightning strike. However, it is questionable if a direct comparison can be made with the current work, as the authors acknowledged their limitation of using narrow specimens (38.1 mm) which could lead to complex finite-width effects and stated that the CAI specimens were mostly used to derive qualitative trends [4]. The larger plate-like CAI specimens used in the current work can resolve this limitation.

Not only are the CAL tests difficult to conduct, but the lightning experiments are also extremely expensive with only a small number of facilities in the world that can apply the high currents used in these tests. In order to effectively study the many parameters involved in both lightning strike and CAL testing our experiments have varied multiple parameters simultaneously and this has allowed us to cover many variables with a small number of specimens. Further study is necessary to systematically study single variables and undertake repeat tests to capture and characterise experimental variation.

There are also some limitations of the current CAL test method. For example, 10 mm of material on each side of the test specimen was not gripped by the test machine, but this was necessary to eliminate the unsupported gap. Otherwise, the upper grips would have interfered with the anti-buckling guides. Justifications can be found from the previous open-hole results [59], in which the slightly wider (120 mm) open-hole specimen not loaded over the complete width shared the same strength scaling trend as the narrower uniformly loaded specimens (100 mm).

6 Conclusions and Future Work

A systematic experimental study has been completed to design a Compression After Lightning Strike (CAL) test method based on the modified Compression After Impact (CAI) test method. Some successful improvements were made to minimise out-of-plane bending due to buckling and an unsupported gap. The current CAL test method is suitable to quantify residual compressive strength for the laboratory lightning strike conditions with a peak current of 25 kA. The 100 kA peak current produced a significantly large internal lightning damage region which made the current specimen dimension (120 mm × 150 mm) and CAL test set-up unsuitable.

Even with a low peak current of 25 kA, the CAL test can capture a compressive failure in the centre of the specimen and a residual strength knock down. It was found that the CAL strength was 28% lower than the pristine CAI strength reported in the literature after a 25 kA peak current strike.

Although this study focuses on the development of the CAL test method, future correlations between internal damage area and the CAL strength will benefit from this robust test method and more repeated tests. The methodology and final test rig used for 25 kA without the unsupported gap could be adapted for both 50 and 75 kA loaded specimens in the future since their compressive failure loads are expected to be lower.

Data Availability The raw/processed data required to reproduce these findings cannot be shared at this time as the data also forms part of an ongoing study.

Declarations

Competing Interest The authors declare that they have no known competing financial interests or personal relationships that could have appeared to influence the work reported in this paper.

Open Access This article is licensed under a Creative Commons Attribution 4.0 International License, which permits use, sharing, adaptation, distribution and reproduction in any medium or format, as long as you give appropriate credit to the original author(s) and the source, provide a link to the Creative Commons licence, and indicate if changes were made. The images or other third party material in this article are included in the article's Creative Commons licence, unless indicated otherwise in a credit line to the material. If material is not included in the article's Creative Commons licence and your intended use is not permitted by statutory regulation or exceeds the permitted use, you will need to obtain permission directly from the copyright holder. To view a copy of this licence, visit <http://creativecommons.org/licenses/by/4.0/>.

References

1. SAE Aerospace.: Aircraft Lightning Environment and Related Test Waveforms (2013). <https://doi.org/10.4271/ARP5412B>
2. EUROCAE.: Aircraft Lightning Environment and Related Test Waveforms 2103
3. Haigh, S.: Impulse Effects during Simulated Lightning Attachments to Lightweight Composite Panels. International Aerospace and Ground Conf. on Lightning and Static Electricity (2007)
4. Feraboli, P., Miller, M.: Damage resistance and tolerance of carbon/epoxy composite coupons subjected to simulated lightning strike. *Compos. Part A Appl. Sci. Manuf.* **40**, 954–67 (2009). <https://doi.org/10.1016/j.compositesa.2009.04.025>.
5. Feraboli, P., Kawakami, H.: Damage of Carbon/Epoxy Composite Plates Subjected to Mechanical Impact and Simulated Lightning. *J Aircr* **47**, 999–1012 (2010). <https://doi.org/10.2514/1.46486>
6. Hirano, Y., Katsumata, S., Iwahori, Y., Todoroki, A.: Artificial lightning testing on graphite/epoxy composite laminate. *Compos. Part A Appl. Sci. Manuf.* **41**, 1461–70 (2010). <https://doi.org/10.1016/j.compositesa.2010.06.008>
7. Kawakami, H.: Lightning Strike Induced Damage Mechanisms of Carbon Fiber Composites. University of Washington (2011)
8. Muñoz, R., Delgado, S., González, C., López-Romano, B., Wang, D.-Y., Llorca, J.: Modeling Lightning Impact Thermo-Mechanical Damage on Composite Materials. *Appl. Compos. Mater.* **21**, 149–64 (2014). <https://doi.org/10.1007/s10443-013-9377-9>
9. Lee, J., Gharghabi, P., Boushab, D., Ricks, T.M., Lacy, T.E., Pittman, C.U., et al.: Artificial lightning strike tests on PRSEUS panels. *Compos. B Eng.* **154**, 467–77 (2018). <https://doi.org/10.1016/j.compositesb.2018.09.016>
10. Mitchard, D., Widger, P., Clark, D., Carr, D., Haddad, A.: Optical emission spectra of high current and high voltage generated arcs representing lightning. *Appl. Phys. Lett.* **114**, 164103 (2019). <https://doi.org/10.1063/1.5092875>
11. Boushab, D., Gharghabi, P., Lee, J., Lacy, T.E., Pittman, C.U., Mazzola, M.S., et al.: Lightning arc channel effects on surface damage development on a PRSEUS composite panel: An experimental study. *Compos. B Eng.* **224**, 109217 (2021). <https://doi.org/10.1016/j.compositesb.2021.109217>
12. Hirano, Y., Yokozeki, T., Ishida, Y., Goto, T., Takahashi, T., Qian, D., et al.: Lightning damage suppression in a carbon fiber-reinforced polymer with a polyaniline-based conductive thermoset matrix. *Compos. Sci. Technol.* **127**, 1–7 (2016). <https://doi.org/10.1016/j.compscitech.2016.02.022>
13. Guo, Y., Xu, Y., Zhang, L., Wei, X., Dong, Q., Yi, X., et al.: Implementation of fiberglass in carbon fiber composites as an isolation layer that enhances lightning strike protection. *Compos. Sci. Technol.* **174**, 117–24 (2019). <https://doi.org/10.1016/j.compscitech.2019.02.023>
14. Wang, B., Ming, Y., Zhu, Y., Yao, X., Ziegmann, G., Xiao, H., et al.: Fabrication of continuous carbon fiber mesh for lightning protection of large-scale wind-turbine blade by electron beam cured printing. *Addit Manuf.* **31**, 100967 (2020). <https://doi.org/10.1016/j.addma.2019.100967>

15. Xia, Q., Zhang, Z., Mei, H., Liu, Y., Leng, J.: A double-layered composite for lightning strike protection via conductive and thermal protection. *Compos. Commun.* **21**, 100403 (2020). <https://doi.org/10.1016/j.coco.2020.100403>
16. Yousefpour, K., Lin, W., Wang, Y., Park, C.: Protection of Carbon Fiber Reinforced Polymer Matrix (CFRP) Composite Laminate Against Lightning Strike Using Nano-Fillers. *IEEE Conference on Electrical Insulation and Dielectric Phenomena (CEIDP)*, 35–38 (2020). <https://doi.org/10.1109/CEIDP49254.2020.9437508>
17. Lin, W., Jony, B., Yousefpour, K., Wang, Y., Park, C., Roy, S.: Effects of Graphene Nanoplatelets on the Lightning Strike Damage Response of Carbon Fiber Epoxy Composite Laminates. *American Society for Composites 2020*, Lancaster, PA: DEStech Publications, Inc. (2020). <https://doi.org/10.12783/asc35/34878>
18. Dong, Q., Wan, G., Guo, Y., Zhang, L., Wei, X., Yi, X., et al.: Damage analysis of carbon fiber composites exposed to combined lightning current components D and C. *Compos. Sci. Technol.* **179**, 1–9 (2019). <https://doi.org/10.1016/j.compscitech.2019.04.030>
19. Wang, F.S., Yu, X.S., Jia, S.Q., Li, P.: Experimental and numerical study on residual strength of aircraft carbon/epoxy composite after lightning strike. *Aerosp. Sci. Technol.* **75**, 304–314 (2018). <https://doi.org/10.1016/j.ast.2018.01.029>
20. Shah, S.Z.H., Lee, J.: Stochastic lightning damage prediction of carbon/epoxy composites with material uncertainties. *Compos. Struct.* **282**, 115014 (2022). <https://doi.org/10.1016/j.compstruct.2021.115014>
21. Lee, J., Lacy Jr., T.E., Pittman Jr., C.U.: Coupled thermal electrical and mechanical lightning damage predictions to carbon/epoxy composites during arc channel shape expansion. *Compos. Struct.* **255**, 112912 (2021). <https://doi.org/10.1016/j.compstruct.2020.112912>
22. Foster, P., Abdelal, G., Murphy, A.: Quantifying the Influence of Lightning Strike Pressure Loading on Composite Specimen Damage. *Appl. Compos. Mater.* **26**, 115–137 (2019). <https://doi.org/10.1007/s10443-018-9685-1>
23. Li, Y., Sun, J., Li, S., Tian, X., Yao, X., Wang, B., et al.: An experimental study of impulse-current-induced mechanical effects on laminated carbon fibre-reinforced polymer composites. *Compos. B Eng.* **225**, 109245 (2021). <https://doi.org/10.1016/j.compositesb.2021.109245>
24. Lee, J., Lacy, T.E., Pittman, C.U.: Lightning mechanical damage prediction in carbon/epoxy laminates using equivalent air blast overpressure. *Compos. B Eng.* **212**, 108649 (2021). <https://doi.org/10.1016/j.compositesb.2021.108649>
25. Millen, S.L.J., Murphy, A., Catalanotti, G., Abdelal, G.: Coupled Thermal-Mechanical Progressive Damage Model with Strain and Heating Rate Effects for Lightning Strike Damage Assessment. *Appl. Compos. Mater.* **26**, 1437–1459 (2019). <https://doi.org/10.1007/s10443-019-09789-z>
26. Millen, S.L.J., Murphy, A.: Understanding the influence of test specimen boundary conditions on material failure resulting from artificial lightning strike. *Eng. Fail. Anal.* **114**, 104577 (2020). <https://doi.org/10.1016/j.engfailanal.2020.104577>
27. Harrell, T.M., Madsen, S.F., Thomsen, O.T., Dulieu-Barton, J.M.: On the Effect of Dielectric Breakdown in UD CFRPs Subjected to Lightning Strike Using an Experimentally Validated Model. *Appl. Compos. Mater.* **29**, 1321–1348 (2022). <https://doi.org/10.1007/s10443-022-10014-7>
28. Hirano, Y., Katsumata, S., Iwahori, Y., Todoroki, A.: Artificial lightning testing on graphite/epoxy composite laminate. *Compos. Part A Appl. Sci. Manuf.* **41**, 1461–1470 (2010). <https://doi.org/10.1016/j.compositesa.2010.06.008>
29. Lee, J., Soutis, C.: Prediction of Impact-Induced Fibre Damage in Circular Composite Plates. *Appl. Compos. Mater.* **12**, 109–131 (2005). <https://doi.org/10.1007/s10443-004-7767-8>
30. Prentzas, V., Tsamasphyros, G.J.: Simulation of Low Velocity Impact on CFRP Aerospace Structures: Simplified Approaches, Numerical and Experimental Results. *Appl. Compos. Mater.* **26**, 835–856 (2019). <https://doi.org/10.1007/s10443-018-9752-7>
31. Bian, T., Lyu, Q., Fan, X., Zhang, X., Li, X., Guo, Z.: Effects of Fiber Architectures on the Impact Resistance of Composite Laminates Under Low-Velocity Impact. *Appl. Compos. Mater.* **29**, 1125–1145 (2022). <https://doi.org/10.1007/s10443-022-10009-4>
32. Featherston, C.A., Eaton, M.J., Evans, S.L., Holford, K.M., Pullin, R., Cole, M.: Development of a Methodology to Assess Mechanical Impulse Effects Resulting from Lightning Attachment to Lightweight Aircraft Structures. *Appl. Mech. Mater.* **24–25**, 129–134 (2010). <https://doi.org/10.4028/www.scientific.net/AMM.24-25.129>
33. Soulas, F., Espinosa, C., Lachaud, F., Guinard, S., Lepetit, B., Revel, I.: Equivalent Impact Set-up for Lightning Strike Damage on Composite Coupons. *International Conference on Composite Materials, Copenhagen, Denmark* (2015)
34. Wang, F.S., Yu, X.S., Jia, S.Q., Li, P.: Experimental and numerical study on residual strength of aircraft carbon/epoxy composite after lightning strike. *Aerosp. Sci. Technol.* **75**, 304–314 (2018). <https://doi.org/10.1016/j.ast.2018.01.029>

35. Wang, F.S., Ding, N., Liu, Z.Q., Ji, Y.Y., Yue, Z.F.: Ablation damage characteristic and residual strength prediction of carbon fiber/epoxy composite suffered from lightning strike. *Compos. Struct.* **117**, 222–233 (2014). <https://doi.org/10.1016/j.compstruct.2014.06.029>
36. Kumar, V., Yokozeki, T., Okada, T., Hirano, Y., Goto, T., Takahashi, T., et al.: Polyaniline-based all-polymeric adhesive layer: An effective lightning strike protection technology for high residual mechanical strength of CFRPs. *Compos. Sci. Technol.* **172**, 49–57 (2019). <https://doi.org/10.1016/j.compscitech.2019.01.006>
37. Kumar, V., Yokozeki, T., Okada, T., Hirano, Y., Goto, T., Takahashi, T., et al.: Effect of through-thickness electrical conductivity of CFRPs on lightning strike damages. *Compos. Part A Appl. Sci. Manuf.* **114**, 429–438 (2018). <https://doi.org/10.1016/j.compositesa.2018.09.007>
38. Guo, Y., Xu, Y., Zhang, L., Wei, X., Dong, Q., Yi, X., et al.: Implementation of fiberglass in carbon fiber composites as an isolation layer that enhances lightning strike protection. *Compos. Sci. Technol.* **174**, 117–124 (2019). <https://doi.org/10.1016/j.compscitech.2019.02.023>
39. Kumar, V., Yeole, P.S., Hiremath, N., Spencer, R., Masum Billah, K.M., Vaidya, U., et al.: Internal Arcing and Lightning Strike Damage in Short Carbon Fiber Reinforced Thermoplastic Composites. *Compos. Sci. Technol.* 112490 (2020). <https://doi.org/10.1016/j.compscitech.2020.108525>
40. Wang, B., Ming, Y., Zhu, Y., Yao, X., Ziegmann, G., Xiao, H., et al.: Fabrication of continuous carbon fiber mesh for lightning protection of large-scale wind-turbine blade by electron beam cured printing. *Addit. Manuf.* **31**, 100967 (2020). <https://doi.org/10.1016/j.addma.2019.100967>
41. Yamashita, S., Hirano, Y., Sonehara, T., Takahashi, J., Kawabe, K., Murakami, T.: Residual mechanical properties of carbon fibre reinforced thermoplastics with thin-ply prepreg after simulated lightning strike. *Compos. Part A Appl. Sci. Manuf.* **101**, 185–94 (2017). <https://doi.org/10.1016/j.compositesa.2017.06.002>
42. Kawakami, H., Feraboli, P.: Lightning strike damage resistance and tolerance of scarf-repaired mesh-protected carbon fiber composites. *Compos. Part A Appl. Sci. Manuf.* **42**, 1247–1262 (2011). <https://doi.org/10.1016/j.compositesa.2011.05.007>
43. Hirano, Y., Yokozeki, T., Ishida, Y., Goto, T., Takahashi, T., Qian, D., et al.: Lightning damage suppression in a carbon fiber-reinforced polymer with a polyaniline-based conductive thermoset matrix. *Compos. Sci. Technol.* **127**, 1–7 (2016). <https://doi.org/10.1016/j.compscitech.2016.02.022>
44. Xia, Q., Zhang, Z., Mei, H., Liu, Y., Leng, J.: A double-layered composite for lightning strike protection via conductive and thermal protection. *Compos. Commun.* **21**, 100403 (2020). <https://doi.org/10.1016/j.coco.2020.100403>
45. Yin, J.J., Li, S.L., Yao, X.L., Chang, F., Li, L.K., Zhang, X.H.: Lightning Strike Ablation Damage Characteristic Analysis for Carbon Fiber/Epoxy Composite Laminate with Fastener. *Appl. Compos. Mater.* **23**, 821–837 (2016). <https://doi.org/10.1007/s10443-016-9487-2>
46. Wang, F.S., Ding, N., Liu, Z.Q., Ji, Y.Y., Yue, Z.F.: Ablation damage characteristic and residual strength prediction of carbon fiber/epoxy composite suffered from lightning strike. *Compos. Struct.* **117**, 222–33 (2014). <https://doi.org/10.1016/j.compstruct.2014.06.029>
47. Kumar, V., Yokozeki, T., Okada, T., Hirano, Y., Goto, T., Takahashi, T., et al.: Effect of through-thickness electrical conductivity of CFRPs on lightning strike damages. *Compos. Part A Appl. Sci. Manuf.* **114**, 429–38 (2018). <https://doi.org/10.1016/j.compositesa.2018.09.007>
48. Kumar, V., Yokozeki, T., Okada, T., Hirano, Y., Goto, T., Takahashi, T., et al.: Polyaniline-based all-polymeric adhesive layer: An effective lightning strike protection technology for high residual mechanical strength of CFRPs. *Compos. Sci. Technol.* **172**, 49–57 (2019). <https://doi.org/10.1016/j.compscitech.2019.01.006>
49. Kumar, V., Yeole, P.S., Hiremath, N., Spencer, R., Billah, K.M.M., Vaidya, U., et al.: Internal arcing and lightning strike damage in short carbon fiber reinforced thermoplastic composites. *Compos. Sci. Technol.* **201**, 108525 (2021). <https://doi.org/10.1016/j.compscitech.2020.108525>
50. Kawakami, H., Feraboli, P.: Lightning strike damage resistance and tolerance of scarf-repaired mesh-protected carbon fiber composites. *Compos. Part A Appl. Sci. Manuf.* **42**, 1247–62 (2011). <https://doi.org/10.1016/j.compositesa.2011.05.007>
51. Abrate, S.: Impact on Laminated Composites: Recent Advances. *Appl. Mech. Rev.* **47**, 517–544 (1994). <https://doi.org/10.1115/1.3111065>
52. McQuien, J.S., Hoos, K.H., Ferguson, L.A., Iarve, E.V., Mollenhauer, D.H.: Geometrically nonlinear regularized extended finite element analysis of compression after impact in composite laminates. *Compos. Part A Appl. Sci. Manuf.* **134**, 105907 (2020). <https://doi.org/10.1016/j.compositesa.2020.105907>
53. Sun, X.C., Hallett, S.R.: Failure mechanisms and damage evolution of laminated composites under compression after impact (CAI): Experimental and numerical study. *Compos. Part A Appl. Sci. Manuf.* **104**, 41–59 (2018). <https://doi.org/10.1016/j.compositesa.2017.10.026>
54. Nettles, A.T., Scharber, L.: The Influence of GI and GII on the compression after impact strength of carbon fiber/epoxy laminates. *J. Compos. Mater.* **52**, 991–1003 (2017). <https://doi.org/10.1177/0021998317119567>

55. Sonehara, T., Kusano, H., Tokuoka, N., Hirano, Y.: Visualization of lightning impulse current discharge on CFRP laminate. *International Conference on Lightning Protection (ICLP)* **2014**, 835–839 (2014). <https://doi.org/10.1109/ICLP.2014.6973239>
56. Yousefpour, K., Chalaki, M.R., Lin, W., Haque, F., Wang, Y., Park, C.: The Impact of Lightning Channel Diameter on the Damage of Carbon Fiber Reinforced Polymer Matrix (CFRP) Composite Laminates. *2020 IEEE Electr. Insul. Conf. (EIC)*, 128–131 (2020). <https://doi.org/10.1109/EIC47619.2020.9158586>
57. Yousefpour, K., Lin, W., Wang, Y., Park, C.: Discharge and ground electrode design considerations for the lightning strike damage tolerance assessment of CFRP matrix composite laminates. *Compos. B Eng.* **198**, 108226 (2020). <https://doi.org/10.1016/j.compositesb.2020.108226>
58. ASTM D7137/D7137M-05.: Standard Test Method for Compressive Residual Strength Properties of Damaged Polymer Matrix Composite Plates. *ASTM Book of Standards* **15(03)**, 18 (2005). https://doi.org/10.1520/D7137_D7137M-05
59. Xu, X., Paul, A., Sun, X., Wisnom, M.R.: An experimental study of scaling effects in notched quasi-isotropic carbon/epoxy laminates under compressive loads. *Compos. Part A Appl. Sci. Manuf.* **137**, 106029 (2020). <https://doi.org/10.1016/j.compositesa.2020.106029>
60. Wisnom, M.R., Hallett, S.R., Soutis, C.: Scaling Effects in Notched Composites. *J. Compos. Mater.* **44**, 195–210 (2009). <https://doi.org/10.1177/0021998309339865>

Publisher's Note Springer Nature remains neutral with regard to jurisdictional claims in published maps and institutional affiliations.